Droplet motion for the conservative 2D Ising lattice gas dynamics below the critical temperature

2001 J. Phys. A: Math. Gen. 34 5901

(http://iopscience.iop.org/0305-4470/34/30/302)

INSTITUTE OF PHYSICS PUBLISHING JOURNAL OF PHYSICS A: MATHEMATICAL AND GENERAL

J. Phys. A: Math. Gen. **34** (2001) 5901–5910 PII: S0305-4470(01)23238-7

Droplet motion for the conservative 2D Ising lattice gas dynamics below the critical temperature

Giorgio Favrin[1], **Enzo Marinari**[2] **and Fabio Martinelli**[3]

[1] Department of Theoretical Physics, Lund University, Sölvegatan 14A, S-22362 Lund, Sweden
[2] Dipartimento di Fisica, INFM and INFN, Università di Roma La Sapienza, PA Moro 2, 00185 Roma, Italy
[3] Dipartimento di Matematica, Università di Roma Tre, Largo S Murialdo 1, 00146 Roma, Italy

E-mail: favrin@thep.lu.se, Enzo.Marinari@roma1.infn.it and martin@mat.uniroma3.it

Received 13 March 2001
Published 20 July 2001
Online at stacks.iop.org/JPhysA/34/5901

Abstract

We consider the 2D Ising lattice gas in a square of side L with free boundary conditions, temperature below the critical one and particle density slightly above the density of the vapour phase. Typical configurations consist of a quarter of a Wulff droplet of the liquid phase centred at one of the corners of the given square. We then introduced a reversible Markovian spin exchange dynamics, also known as Kawasaki dynamics, on the configuration space and we discuss the heuristics of the transition of a bubble of the liquid phase from one corner to another. We then present some numerical evidence suggesting that the preferred mechanism to make the transition is via evaporation of the original bubble and simultaneous reconstruction of a new bubble around a new corner.

PACS numbers: 05.50.+q, 05.10.Ln, 63.70.+h, 64.60.Kw, 75.10.-b

(Some figures in this article are in colour only in the electronic version)

1. Introduction

The problem of computing the relaxation time of stochastic Monte Carlo algorithms for models of lattice classical spin models has attracted in the last years considerable attention and many new rigorous techniques have been developed, giving rise to nice progress in probability theory and statistical mechanics. If for simplicity we confine ourselves to ± 1 (or 0, 1 in the lattice gas picture) spins, the two most studied random dynamics have been non-conservative Glauber type algorithms, in which one spin at a time flips its value with a rate satisfying the detailed balance condition with respect to the grand canonical Gibbs measure, and conservative Kawasaki dynamics in which nearest-neighbour spins exchange their values with a rate satisfying the detailed balance condition with respect to the canonical Gibbs measure.

0305-4470/01/305901+10$30.00

A warning sign is in order here. Most of the rigorous results presented below have been obtained in the 'continuous time' setting, namely when the stochastic dynamics is a continuous time Markov chain and the time units are such that, in a unitary time interval, on average every spin tries to change its value once. In the physics literature, but also in the Markov chain Monte Carlo approach to computational problems and image reconstruction, the discrete time setting in which at each time step only one dynamical variable is updated is more familiar. In most cases the simple rule to translate results from one case to another is to multiply by the appropriate change of scale, but sometimes subtle problems may appear in the discrete setting (see e.g. [1]).

Let us go back to a quick review of the main results. For Glauber dynamics in the one-phase region the general picture is relatively clear for a wide class of models and the conclusion is that equilibrium is reached exponentially fast provided certain mixing assumptions are satisfied by the grand canonical Gibbs measure (see e.g. [2] and references therein). In the conservative case, instead, the basic results [3, 4] and more recently [5], state that, at high temperature, the relaxation time in a box of side L grows as L^2 (diffusive scaling).

A natural question arises as to what happens when the thermodynamic parameters (e.g. inverse temperature and the external magnetic field in the Glauber case or inverse temperature and particle density in the conservative case) are such that we do have a phase transition in the thermodynamic limit.

Let us start with the Glauber case and, to be concrete, let us consider the usual Ising model in a two-dimensional box V of side L, without external field, and inverse temperature β larger than the critical value β_c. With free boundary conditions the picture of the relaxation behaviour to the Gibbs equilibrium measure that emerges is the following. The system first relaxes rather rapidly to one of the two phases and then it creates, via a large fluctuation, a thin layer of the opposite phase along one of the sides of V. Such a process requires an average time of the order of $\exp(\beta\tau_\beta L)$, where τ_β denotes the surface tension in the direction of one of the coordinate axes. After that, the opposite phase invades the whole system by moving, in a much shorter timescale, the interface to the side opposite to the initial one and equilibrium is finally reached. The time required for this final process can be computed to be of the order of L^3 at least in the SOS approximation (see [6]).

Let us now turn to the much more involved conservative case in the same setting (low temperature and free boundary conditions). Here results are much less precise (see [7]).

Let us denote by N the total number of particles in V and let us assume that $\rho \in (\rho_-^*, \rho_+^*)$, where ρ and $\rho_\pm^*$ denote the actual density and the density of the liquid/vapour phases respectively. With these assumptions it can be shown that the relaxation time is again exponentially large in L but, in contrast to the conservative case, almost nothing is known rigorously about the exact constant in the exponential and about the physical mechanisms behind equilibration.

That the relaxation time is very large can be easily understood (but painfully proved) by the following reasoning. Assume for simplicity that ρ is slightly above ρ_-^* in such a way that, typically, the gas at equilibrium shows phase segregation between a (macroscopically) small bubble of liquid immersed in vapour. Because of the free boundary conditions the bubble prefers to sit around one of the corners of V. Clearly, in order to reach equilibrium, the system started as above has to move the bubble to the other corners but, in doing that, it is forced to explore a region of the phase space of exponentially (in L) small canonical probability (and that is the hard part in a rigorous approach). In other words it seems clear that the slowest mode in the dynamics comes from the corner to corner droplet transport. A precise understanding of the above motion appears therefore to be an interesting problem on its own and almost unavoidable if one wants to quantify precisely the relaxation time. A first numerical attempt

in this direction represents the main goal of this paper, which is in turn based on the work contained in [8].

We conclude by observing that, if boundary conditions are changed to for example plus or periodic, then the whole scenario changes drastically and one may argue that the slowest mode of the system is associated with the random walk motion of the centre of gravity of the unique Wulff bubble of the liquid phase. If that is true then simple heuristics shows that the relaxation time should now grow as L^3 (in continuous time units) or L^5 in discrete time steps.

2. Model and notation

We define here our model and notation.

2.1. Equilibrium probability measures

We consider the two-dimensional lattice $\boldsymbol{Z}^2$ with *sites* $x = (x_1, x_2)$. By Q_L we denote the square of all $x = (x_1, x_2) \in \boldsymbol{Z}^2$ such that $x_i \in \{0, \ldots, L-1\}$, $i = 1, 2$. The *edges* of $\boldsymbol{Z}^2$ are those $e = [x, y]$ with x, y nearest neighbours in $\boldsymbol{Z}^2$. Given $V \subset \boldsymbol{Z}^2$, we denote by $\mathcal{E}_V$ the set of all edges such that both endpoints are in V.

The configuration space. Given $V \subset \boldsymbol{Z}^2$, our *configuration space* is $\Omega_V = S^V$, where $S = \{-1, 1\}$. Sometimes the *lattice gas* point of view will be more convenient, so we also consider the space $\Omega'_V = \{0, 1\}^V$ and its natural one-to-one correspondence with Ω. We define the *unnormalized magnetization* $M_V : \Omega_V \mapsto \boldsymbol{Z}$ and the *number of particles* $N_V : \Omega'_V \mapsto \boldsymbol{N}$ as

$$M_V(\sigma) = \sum_{x \in V} \sigma(x) \qquad N_V(\eta) = \sum_{x \in V} \eta(x) \tag{1}$$

while the *normalized magnetization* is given by $m_V = M_V/|V|$.

The interaction and the Gibbs measures. Given a finite set $V \subset \boldsymbol{Z}^2$ we define the Hamiltonian with free boundary condition $H_V : \Omega_V \mapsto \boldsymbol{R}$ by

$$H_V(\sigma) = -\sum_{[x,y] \in \mathcal{E}_V} \sigma(x)\sigma(y)\,. \tag{2}$$

The corresponding (finite-volume) Gibbs measure is given by

$$\mu_V^\beta(\sigma) = \left(Z_V^\beta\right)^{-1} \exp[\,-\beta H_V(\sigma)\,] \tag{3}$$

where Z_V^β is the proper normalization factor, called the partition function. We denote by $m^*(\beta)$ and β_c the *spontaneous magnetization* and *inverse critical temperature* of the two-dimensional Ising model respectively. It is well known that $\beta_c = (1/2)\log(1+\sqrt{2})$. The density of the liquid and the vapour phase, denoted respectively by $\rho_+^*(\beta)$ and $\rho_-^*(\beta)$, can be expressed as $\frac{1}{2}(1 \pm m^*)$.

We also introduce the *canonical Gibbs measure* defined as

$$\nu_{V,N}^\beta = \mu_V^\beta(\cdot \mid N_V = N) \qquad N \in \{0, 1, \ldots, |V|\} \tag{4}$$

where N_V is the number of particles in V.

3. The Kawasaki dynamics

Here we define the relevant Markovian dynamics, reversible with respect to the canonical Gibbs measure, that will be used and analysed in the rest of this paper.

Given $V \subset \mathbb{Z}^2$, $b \in \mathcal{E}_V$ and a particle configuration $\eta \in \Omega'_V$ (equivalent to a spin configuration $\sigma \in \Omega_V$), let η^b be the configuration obtained from η by interchanging the values of the η variables at the end points of the bond b. The energy difference between the two configurations is given by

$$\Delta_b H_V(\eta) \equiv H_V(\eta^b) - H_V(\eta). \tag{5}$$

If $\eta^b \neq \eta$ we call b a *broken bond* and we say it belongs to $\mathcal{B}_\eta$. With the above notation the Kawasaki dynamics with Metropolis transition probability matrix is given by:

$$W(\eta, \eta') = \begin{cases} \dfrac{1}{|\mathcal{E}_V|} \mathrm{e}^{-\beta \max(0, \Delta_b H_V(\eta))} & \text{if} \quad \eta' = \eta^b \qquad \text{and} \qquad b \in \mathcal{B}_\eta \\ 1 - \displaystyle\sum_{b \in \mathcal{B}_\eta} W(\eta, \eta^b) & \text{if} \quad \eta' = \eta \\ 0 & \text{otherwise.} \end{cases} \tag{6}$$

Clearly, for each $N \in [1, |V| - 1]$, W describes an ergodic Markov chain on the configuration space $\Omega'_{V,N}$, which consists of all particle configurations with particle number equal to N. In particular, since W satisfies the detailed balance condition with respect to the canonical measure $\nu^\beta_{V,N}$, the latter coincides with the unique invariant measure of the chain.

4. Corner to corner matter transport

In this section we will first try to define our field of investigation by starting with a discussion of the typical configurations for the canonical measure of the Ising model below the critical temperature with free boundary conditions. We will then analyse some possible mechanisms for the corner to corner bubble transition, and the typical timescales that govern the process. Subsequently we will discuss the details of our numerical simulations and give some hints about the updating algorithm. Finally we will present the main results of this note.

4.1. Heuristics

Let $V = Q_L$, let $\rho \in (\rho^*_-, \rho^*_+)$, where $\rho^*_\pm$ have been defined above, and let $N = \lfloor \rho L^2 \rfloor$ be the total number of particles.

For the above situation, it is useful to recall first the shape of the typical configurations of the canonical Ising Gibbs measure with free b.c. when the temperature is below the critical value and L is very large.

Let $m_\rho = 2\rho - 1$ be the usual magnetization associated with the given particle density. Then, as discussed in [10] and [9], there exists $0 < m_1(\beta) < m^*(\beta)$ such that

(i) if $m_\rho \in (-m_1, m_1)$ then the typical configurations show phase segregation between a high-density ($\approx \rho^*_+$) region and a low-density ($\approx \rho^*_-$) region that are roughly two horizontal (or vertical) rectangles of appropriate area separated by a horizontal (or vertical) interface of length $\approx L$ and

(ii) if $m_\rho \in (-m^*(\beta), -m_1(\beta)] \cup [m_1(\beta), m^*(\beta))$ then the typical configurations show phase segregation between a high-density ($\approx \rho^*_+$) region and a low-density ($\approx \rho^*_-$) region, the smaller of which is a quarter of a Wulff shape (see [12]) of appropriate area and it is centred in one of the four vertices of Q_L. For the reader's convenience we recall that a Wulff shape is, at very low T, very similar to a perfect square.

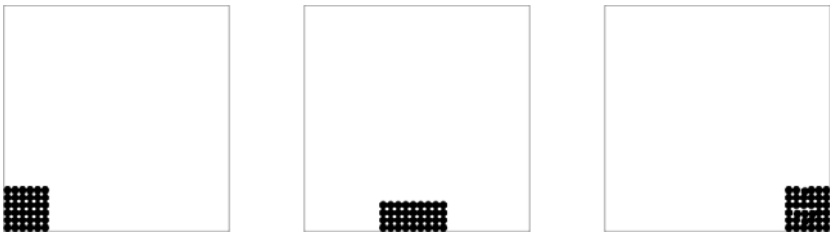

Figure 1. The sliding motion of the bubble, from the left to the right bottom corner.

What is important for us is that in both cases the typical configurations of the canonical measure show a discrete symmetry described by rotations of $k\frac{\pi}{2}$, $k = 0, 1 \ldots$ around the centre of Λ. As a consequence, if the dynamics starts from one typical configuration for which for example the particles form a cluster in a corner (this is one of the situations we have described before), then, in order to reach equilibrium, it must necessarily cross an unlikely region in the configuration space. One can show that the canonical probability of such region is exponentially small in L [7]. Therefore a bottleneck is present in the configuration space, and the relaxation time is exponentially large in L [7].

In the sequel to this paper we will always assume that we are in the second of the two scenarios described above, and in particular we will assume that m and ρ are respectively larger than but quite close to the values $-m^*(\beta)$ and $\rho^*_-(\beta)$. In other words we are considering a situation in which typically the particles form a small (on a macroscopic scale) cluster of a specific shape around one of the four corners of Λ. Clearly we do not mean that all the particles that are in Λ are in the bubble, and we do not mean that the bubble does not have empty holes in its interior. What we mean exactly is that, with high probability, there exists a macroscopic region with a precise shape around one of the corners where the particle density is very close to the density of the liquid phase, ρ^*_+ (corresponding to the Onsager magnetization density).

Next we analyse some possible mechanisms for the corner to corner bubble transition, namely the process that moves the liquid bubble from one corner to a different one.

We can see two main mechanisms that could intervene.

The first one involves a deformation of the initial Wulff droplet, that for simplicity we will assume here and in the following to be a square of side B (where $\rho L^2 = \rho^*_+ B^2 + \rho^*_-(L^2 - B^2)$) and with one vertex sitting on the left lower corner of Λ, into a rectangle. We call this case *sliding*. We can describe it as follows: we assume that the particles always (that is also during the transition to one of the other corners) form one compact cluster (apart from the usual small fluctuations) that, based on energetic considerations, we can assume to be a generic rectangle $\mathcal{R}$ of sides B_1 and B_2. Energetically, because of the free boundary conditions, at equilibrium it will find it convenient to be a square of side B attached to two sides of Λ. Under the Kawasaki dynamics we can imagine that such a square is deformed, by some sort of matter transport along the boundary, until it reaches the shape of a rectangle $\mathcal{R}^*$ of sides $B_1 > B_2$ (B_1 being the horizontal side) with the left and bottom sides attached to the boundary of Λ. At this point the rectangle $\mathcal{R}^*$ begins to slide along for example the bottom side of Λ until it reaches the opposite corner, where it deforms back to the original square (see figure 1). The energy barrier ΔH one has to cross in this process is clearly of the order of $2(B_1 + 2B_2) - 2(2B)$ at least at very low temperature. If we now optimize over B_1 and B_2 under the constraint that $B_1 \times B_2 = B^2$ we obtain $B_1 = \sqrt{2}B$ and $B_2 = \frac{1}{\sqrt{2}}B$. Thus $\Delta H = 4(\sqrt{2} - 1)B$ and therefore we expect that the average time to see a *sliding* transition will be of the order of $t_{\text{sliding}} \approx \exp(\beta \Delta H)$.

The second mechanism that one can imagine is what we call *evaporation*. Particles individually separate from the liquid bubble (they evaporate) and start to perform a sort of random walk in the vapour phase (typically along the boundaries, for energetic reasons). Clearly the excess particles in the vapour phase prefer, as soon as they can, to gather together around one of the nearby corners, and grow there a new liquid bubble. Typically these trial bubbles do not achieve a macroscopic volume, but die long before reaching this stage and their particles end up returning to their mother bubble. Only rare fluctuations lead to more than half of the particles clustering together: in these cases typically the new bubble will form in the selected corner, and evaporation will continue until all the original liquid bubble has been reformed around the new corner (clearly particles of the bubble are interchanged at all moments with particles that are in equilibrium in the vapour phase). It is not difficult to check that, at least to leading order, the energy barrier is crossed when the two groups of particles in the two different corners have the same volume (and same Wulff shape). At very low temperature we obtain immediately that $\Delta H = 4(\sqrt{2} - 1)B$, exactly as in the former case.

We conclude this part by stressing that all the above reasonings were based only on energy barrier considerations and that we have never taken into account entropic contributions. The latter may play an important role in selecting one mechanism instead of another. Moreover prefactors in the typical timescales of each process may also be relevant and in that case a more detailed analysis would be required.

4.2. Numerical simulations

Our experimental setting can be described as follows: we use a square two-dimensional lattice with free boundary conditions. We have investigated lattice sizes from $L = 20$ to 30. The inverse temperature β has been assigned the two values $\beta = 0.7$ and 1.05 in different cases (this is of the order of twice the value of the inverse critical temperature β_c). Finally we have chosen the number of particles in the range 25–36 (corresponding to initial conditions with a bubble of 5×5 or 6×6 particles in a corner of the square lattice). Notice that in our range of temperatures the density of the vapour ρ_-^* lies between 5×10^{-3} and 2×10^{-4} for the two different temperature values: in other words we are in extreme conditions.

The updating algorithm is of course based on the transition matrix (6), and goes as follows. We consider the particle configuration at time t, $\eta(t)$. We select a broken bond (that is a bond in the set $\mathcal{B}_{\eta(t)}$) at random, with uniform probability. We compute the energy difference $\Delta_b H_V(\eta(t))$ defined in (5): if it is negative we accept the update proposal, and set $\eta(t+1) = \eta^b(t)$. Otherwise we accept the update proposal with probability $\exp(-\beta \Delta_b H_V(\eta(t)))$, and refuse it otherwise, setting in this case $\eta(t+1) = \eta(t)$.

This procedure, while appealing from the point of view of the computational efficiency, and satisfactory from the physical point of view, does not satisfy detailed balance, since the number of broken bonds is not a conserved quantity (see for instance the discussion in [11]). In our working conditions, however, this effect is very small and, as far as many issues are concerned, irrelevant. In fact, as we have already explained, we will mostly focus on the mechanisms on which the bubble transition is based: since the small violation of detailed balance amounts to watching a movie that runs at slightly variable speed, spatial phenomena (for example what the transition path of the bubble is or what its typical spread is during the transition) are described in an exact manner. Scaling arguments (for example the scaling of the transition time with β) could as matter of principle be sensitive to the violation of detailed balance: we believe however that only the prefactors will be affected, and all of the many tests of universality that we have performed on our simulations confirm this point of view.

We still have to discuss the criterion by which we define a bubble transition. We have

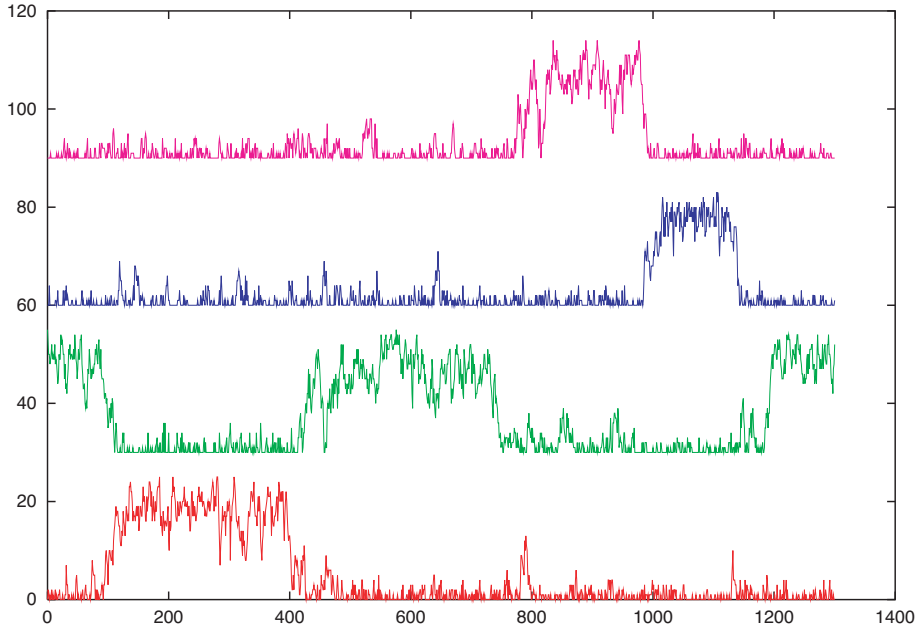

Figure 2. The number of particles close to each of the four corners as a function of time. See the text for further details.

indeed used two different criteria and checked that in the two cases we obtain consistent results. In the first scheme we define four boxes, with a vertex in one of the four corners, with an area equal to that of the original bubble (that starts, let us say, from the top left corner). We then define a transition as the event where the centre of mass of the particles that constitute the bubble enters a new box. In the second scheme we define a transition as the event where three-quarters of the particles have left the initial box: since we expect to have a transition when half of the particles have left, we are confident that 75% is a safe signal for a transition. Numerical simulations will confirm the coincidence of the two criteria.

5. Results and discussion

In figure 2 we show the number of particles (modulo a corner-dependent offset needed to make the figure readable) at time t near the four different corners of the lattice during the course of the dynamics. More precisely we have defined square boxes of size B^2 with a vertex in each of the four corners, where B^2 is the total number of particles (25 in the present case) and for each box we have computed the time history of the number of particles inside the box, under the condition that at time $t = 0$ all the particles are in the leftmost bottom box. The value for the lowest curve (representing one given corner) is exactly the value of the number of particles in the corner, while the other three curves have an offset of, respectively, 30, 60 and 90 for the three different corners. The transitions are always abrupt, and the particles spend the quasi-totality of their time confined in one corner. As one expects on theoretical grounds the typical time scale on which a transition occurs is much shorter than the time one has to wait to see the transition. The system is waiting for a *critical fluctuation*, making many unsuccessful attempts (the small spikes towards the bottom of the figure).

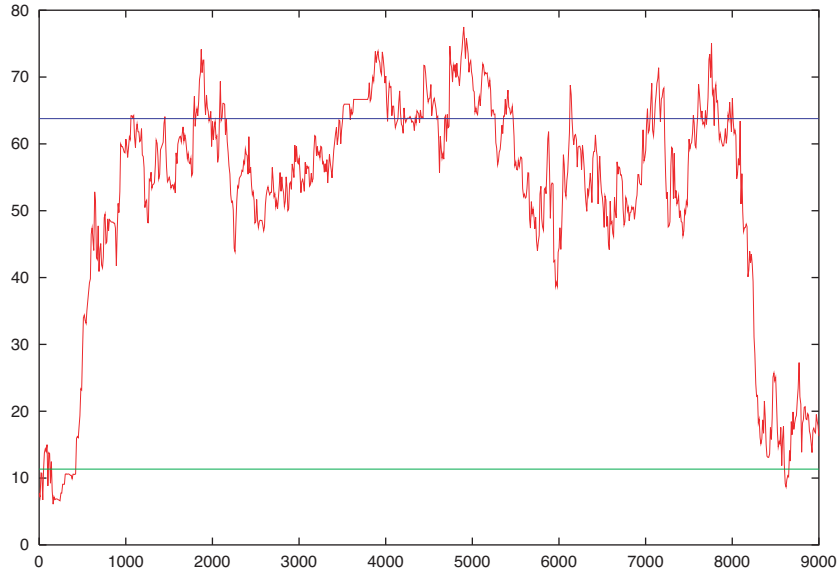

Figure 3. Variance of the centre of mass as a function of the time.

In figure 3 instead we have computed the 'variance' of the centre of mass of the particles. We define

$$\sigma^2(t) \equiv \frac{1}{B^2} \sum_i \left(x_i(t) - x^{(\mathrm{cm})}(t)\right)^2 \tag{7}$$

where $x_i(t)$ are, as usual, the positions of the particles on the two-dimensional square lattice, and $x^{(\mathrm{cm})}(t)$ is the centre of mass of the particles at time t. We compare it to the two extreme situations, where the particles form a compact blob (the lowest straight line), and where the particles are divided into two, equal sized, compact blobs in two adjacent corners (see the previous discussion in section 3.1). The timescale of this figure (in arbitrary units again) is much smaller than that of the previous figure, and basically gives the time of a single transition. In other words we have analysed the time behaviour of the above variance precisely during the short (in the timescale of figure 2) time interval in which the transition takes place. The outcome is that the particles go from a compact blob (in a corner) to a compact blob (in a different corner) passing through a situation where they are basically divided into two groups of similar size.

The second part of our analysis considers scaling behaviours of the (average) transition times $T(\beta, L)$. We look separately at the dependence of T over β and over the size L. In figure 4 we look at the β dependence over the range $[0.65, 1.1]$ for a fixed side $L = 20$ (and 25 particles). Our best fit to the form

$$T(\beta) = A\, \mathrm{e}^{\beta \delta H} \tag{8}$$

is very good and gives $\Delta H \simeq 17.8$ (and $A \simeq 0.001$).

This is in very good agreement with the heuristic calculation of the energy barrier assuming that the transition occurs via the mechanism we have called *evaporation*, that suggests that ΔH is of the order of 20. We illustrate the mechanism in figure 5. We start with 25 particles packed in the left down-most corner: here the surface includes 10 broken links. Now in the intermediate situation of figure 5, that is a typical intermediate particle configuration, we have

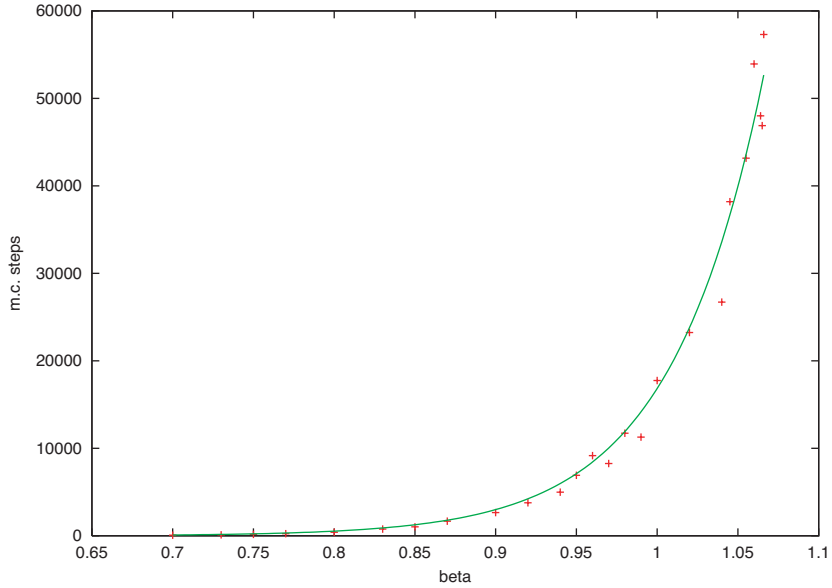

Figure 4. Transition time as a function of β.

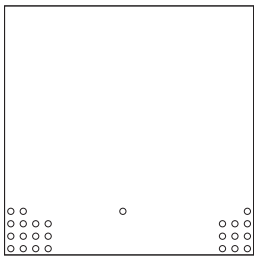

Figure 5. The dynamical mechanism we call *evaporation*. See the text for further details.

19 broken links. Clearly it would be less expensive for the lonely particle to travel along the side of the lattice, but the configuration we show has a higher entropy and we observe these kinds of process with high frequency. Since ΔH is equal to twice the difference in the number of broken links, in this case $\Delta H = 18$. This is only an estimate, but gives the correct order of magnitude. Notice that $\Delta H = 18$ is quite far from the infinite-volume saddle we have discussed before, that would give $\Delta H = 4(\sqrt{2} - 1)B \simeq 8$: this is due to finite-size effects (both B and L are finite). We have verified that when we change the number of particles (for example from 25 to 36) or the definition of a *transition* from corner to corner we continue to find the expected scaling behaviour.

6. Conclusions

In this paper we have investigated, mainly numerically, the Kawasaki dynamics (a particular conservative particle–hole exchange) for the low-temperature ($\beta \approx 2\beta_c$) Ising lattice gas in a box with free boundary conditions and side $L \approx 30$. The number of particles N has been chosen in a such a way that phase segregation occurs (typically $N \approx 25$). With the above

choice of the thermodynamic parameters the typical equilibrium configurations consist of a (small compared to the total volume) squarelike droplet of particles which sits in one of the four corners because of the chosen boundary conditions and a rarefied gas elsewhere. Under the Kawasaki dynamics the droplet of particles makes rare and mostly unsuccessful attempts to migrate to one of the empty corners. Based on energetic considerations alone, thus neglecting entropic contributions, we have envisaged two main best possible mechanisms for the migration to take place, that we have named *sliding* (the bubble of particles is deformed into a rectangle, slides along one side of the box until it reaches the opposite corner and finally reconstructs the optimal squarelike shape) and *evaporation* (the particles in the bubble evaporate into the rarefied gas and recollect together to a form a new bubble in another corner) respectively. We have then performed intensive numerical investigation to check whether sliding or evaporation is the prefered mechanism and the scaling behaviour with the inverse temperature β of the (average) transition time. Under various different definitions of the bubble transition our results consistently indicate that *evaporation* is the dominant effect and that the scaling law for the average transition time $T(\beta)$ is of the form

$$T(\beta) = A\,\mathrm{e}^{\beta\delta H} \tag{9}$$

where the energy barrier δH is in very good agreement with simple energetic considerations.

References

[1] Frigessi A, Martinelli F and Stander J 1997 Computational complexity of Markov chain Monte Carlo methods for finite Markov fields *Biometrika* **84** 1

[2] Martinelli F 2000 Lectures on Glauber dynamics for discrete spin models *Lecture Notes in Mathematics* vol 1717 (Berlin: Springer)

[3] Sheng-Lin Lu and Yau H-T 1993 Spectral gap and logarithmic Sobolev inequality for Kawasaki and Glauber dynamics *Commun. Math. Phys.* **156** 399

[4] Yau H-T 1996 Logarithmic Sobolev inequality for lattice gases with mixing conditions *Commun. Math. Phys.* **181** 367

[5] Cancrini N and Martinelli F 2000 On the spectral gap of Kawasaki dynamics under a mixing condition revisited *J. Math. Phys.* **41**

[6] Posta G 1995/97 Spectral gap for an unrestricted Kawasaki type dynamics *ESAIM Prob. Stat.* **1** 145

[7] Cancrini N, Cesi F and Martinelli F 1999 Kawasaki dynamics at low temperature *J. Stat. Phys.* **95** 219

[8] Favrin G 1999 Nuovi risultati sulla dinamica di Kawasaki *Tesi di Laurea* Cagliari University

[9] Cesi F, Guadagni G, Martinelli F and Schonmann R 1996 On the 2D stochastic Ising model in the phase coexistence region near the critical point *J. Stat. Phys.* **85** 55

[10] Shlosman S B 1989 The droplet in the tube: a case of phase transition in the canonical ensemble *Commun. Math. Phys.* **125** 81

[11] Shida C S and Henriques V B 2000 Kawasaki dynamics and equilibrium distributions in simulations of phase separating systems *Int. J. Mod. Phys.* C **11** 1033
(Shida C S and Henriques V B 1997 *Preprint* cond-mat/9703198)

[12] Dobrushin R, Kotecký R and Shlosman S 1992 Wulff construction. A global shape from local interaction *Translation of Math. Monographs* vol 104 (Providence, RI: American Mathematical Society)